Step Climbing Cooperation Primitives for Legged Robots with a Reversible Connection

Carlos S. Casarez[1] and Ronald S. Fearing[2]

***Abstract*— Cooperation primitives for climbing steps were developed for a system of two 10 cm long VelociRoACH hexapedal legged robots with a removable connection. When performed sequentially, the set of primitives allow the team of two robots to climb a step on the order of their body length. These primitives use a tether between the robots actuated by a winch on one of the robots to form and release connections, run synchronously while connected, and provide a tether assist force while running. For a step with a coefficient of friction of 1 and a height of 6.5 cm, quasi-static analysis correctly predicts that the two connected robots can raise the front robot over the top of the step, while a single robot can only pitch upward against the step. The winch module designed to perform the cooperative climbing experiments meets the system goals of providing controllable forces greater than each robot's body weight while driving a removable connection between the robots. Experiments demonstrate that the robot system can perform each cooperation primitive individually with a reliability of at least 50% using simple strategies of maintaining a constant bounding frequency with the drive motors of each robot and a set tether tension with the winch.**

I. Introduction

Small bio-inspired robots have the potential to improve the effectiveness of robot-assisted search and rescue in disaster scenarios (e.g. collapsed buildings). Small-scale robots can navigate through narrow spaces in a collapsed building that would be otherwise inaccessible. Furthermore, these robots can be produced cheaply and quickly through the scaled Smart Composite Microstructures (SCM) process [1]. The maneuverability and ease of manufacture of SCM robots allows them to be deployed in large numbers (10-100 units). Deploying many capable and low-cost robots throughout the disaster area will help to localize sites that are viable entry points for rescuers, accelerating the discovery and rescue of survivors.

While underactuated, bio-inspired legged robots have demonstrated high-speed running performance on level ground with some obstacles [2] and turning maneuverability through both differential drive [3] and roll oscillations from phase-locked gaits [4], their use beyond controlled laboratory settings has been limited. These limitations are inherent to underactuated legged locomotion–including not being able to control individual leg articulation and contact forces. As a result, climbing over step obstacles that are larger than the robot's length scale poses a great challenge for an individual robot. We posit that through multi-robot physical cooperation, small legged robots can approach the locomotion capabilities of animals, such as Australian jumping ants, which are shown cooperatively traversing complex terrain in the attached video.

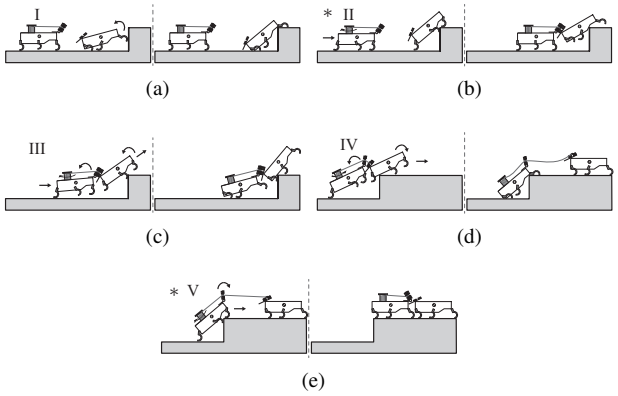

Fig. 1. Diagram illustrating the primitives (I,...,V) of cooperative step climbing with an active tether: (a) I: front robot transitions from horizontal to pitched up against the wall, (b) II: back robot reels in the tether to retain connector and forms a compliant pin connection with the front robot, (c) III: connected robots locomote synchronously, (d) IV: back robot reels out the tether and front robot climbs over step with connector attached, (e) V: back robot reels in the tether while climbing over step and retrieves the tethered connector. The starred primitives are not accompanied by supporting analysis.

The goal of this paper is to demonstrate that simple connections between underactuated legged robots can enable mobility over tall obstacles relative to their size, with no specialized attachment mechanism required. This physical cooperation to overcome obstacles is represented in the concept diagram in Fig. 1. The addition of a tensile winch element and a compliant connection interface allows the robots to form reconfigurable connections. The compliant pin connection between the robots allows the back robot to assist the front robot to the top of the step through pushing forces and restoring spring moments that resist pitching backwards. The front robot can then successfully climb the step by releasing the connection and walking forward. Additionally, if the front robot has sufficient traction once it climbs the step, the tensile force of the active tether between the robots can assist the back robot in overcoming the step. The system benefits from the reconfigurability of the connection because the tethered connector can be used in connected climbing and

*This material is based upon work supported by NSF IGERT Grant No. DGE-0903711, NSF CMMI Grant No. 1427096, and the United States Army Research Laboratory under the Micro Autonomous Science and Technology Collaborative Technology Alliance.

[1]Carlos S. Casarez is with the Department of Mechanical Engineering, University of California, Berkeley, CA 94720 USA. casarezc@berkeley.edu

[2] Ronald S. Fearing is with the Department of Electrical Engineering and Computer Sciences, University of California, Berkeley, CA 94720 USA. ronf@eecs.berkeley.edu

tether-assisted climbing modes but can also be retrieved by the back robot using the winch.

The paper is organized as follows: Section II reviews the recent literature on robots that overcome obstacles through specialized climbing mechanisms, modular design, environment modification, and tether interactions, and places this research in the context of the previous work. Section III presents a quasi-static planar analysis that gives friction limits on step climbing for either a single robot or two connected robots. Section IV describes the components of the system of VelociRoACH (Velocity Robotic Autonomous Crawling Hexapod) robots with reconfigurable compliant connections and details the experimental reliability of each cooperative climbing primitive when performed independently. Section V discusses the application of the results to general design principles and the implementation of real-world obstacle navigation for this type of cooperative robot system.

II. Background

To traverse obstacles, many robots use specialized climbing mechanisms. Using claws or spines, CLASH [5], RiSE [6], and DynoClimber [7] have demonstrated vertical climbing on penetrable or rough surfaces. Also, several robots climb smooth vertical surfaces with gecko adhesives, such as Stickybot [8], CLASH [9], and Waalbot I and II [10], [11]. Power plant robots tailored to steam chests, generators, and boiler tubes use magnetic attachment to metal surfaces [12]. These robots all climb specialized surfaces, and only the Waalbot demonstrated the ability to climb steps by making horizontal to vertical transitions.

More unique strategies for climbing obstacles have also been explored–Hand-bot as part of a heterogeneous team can climb up bookshelves, but has no individual mobility [13]. RHex can employ a bio-inspired step climbing gait strategy to climb over steps more than twice its leg length [14].

Another approach to climbing obstacles is to use connected modules with distributed actuation. Deshpande showed that force cooperation between tracked modules can reduce friction required and prevent tipping while climbing obstacles [15]. Similarly, Shoval and Shapiro demonstrated a 6-DOF semi-passive linkage connecting tracked modules that improves slope-climbing ability [16].

Some modular robots that climb steps with drive and joint actuation include the Souryu robots [17] and tracked modules by Liu [18]. Other modular robots climb steps with active drive elements and passive joints, including wheel modules by Avinash [19], and the Genbu robot [20]. Modular robots that strike a balance between these two extremes and have actuation away from joints include the snake-like robot with cable articulation of modules by Ito [21], and the tank-like modular robot with active tail by Seo [22]. Modular robots can overcome step obstacles because of advantages such as body articulation and distributed drive elements, but sacrifice the mobility advantages of individual modules in many cases because they are permanently connected.

Environment modification is an approach that builds over the obstacle instead of addressing it directly. Some examples include Termes robots that build structures with blocks [23], and dispensing amorphous foam ramps by Napp [24]. Environment modification is easily scalable for multi-robot cooperation, but requires a large payload of structures or dispensing sources.

Tether cooperation between robots has also proven to aid mobility. Mumm et al. showed how a wheeled robot can traverse a slope using active tethers attached at the top of the slope [25]. The Dante II robot with an anchored actuated tether could more easily traverse steep and rocky terrain [26]. The Axel and DuAxel rovers performed similar tether-assisted climbing, but with independent modules that can be separated [27]. SPIDAR demonstrated the utility of an actuated tether in a search and rescue scenario by having a human deploy and retrieve the robot with the tether [28]. These active tether robots start at the top of a cliff or obstacle, even though the modules do not have the capability to climb the obstacle unassisted. In the exploration of an unstructured environment such as a building collapse site, this may not be a valid assumption and hence we need to address obstacle climbing as well as assisted ascent/descent.

The cooperation primitives in Fig. 1 draw from established methods of using connected modules and tether assistance to improve obstacle traversal capability. By using minimal connection components and a single actuator to form connections, provide tether pulling assistance, and remove connections between robots, the proposed robot system improves the step climbing performance of the team while retaining the individual mobility of the modules.

III. Analysis of cooperative step climbing

The cooperative step climbing behavior can be divided into the five primitives illustrated in Fig. 1. The back robot has a winch module that pulls a tether attached to a magnetic connector, which facilitates interaction with the front robot. In primitive I (Fig. 1a), the front robot uses a bounding gait to partially climb the step and change its inclination angle from horizontal to a final resting value. In primitive II (Fig. 1b), the back robot approaches the front robot while reeling in the tether to retain the magnetic connector, the front robot postures its legs backwards to raise the connection point, and the robots join magnetically to form a compliant pin connection. In primitive III (Fig. 1c), the connected robots cooperatively locomote with bounding gaits to raise the center of mass of the front robot above the edge of the step. In primitive IV (Fig. 1d), the back robot disengages the pin connection by reeling out the tether and pitching upward. The front robot then walks forward to an anchor point on top of the step, with the tethered magnetic connector still attached. In primitive V (Fig. 1e), the back robot reels in the tether while using a bounding gait to climb over the step. The tethered magnetic connector is then retrieved by the back robot by applying a sufficiently large force with the winch.

In the following quasi-static analysis, we use a single rigid body model of the robot in the sagittal plane to determine limits on step climbing. Assuming friction-limited

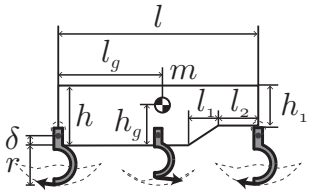

Fig. 2. Diagram of the three leg single rigid body model of the robot in the sagittal plane. The leg configuration is shown for the fixed crank angle $\phi = 90^\circ$ used in the quasi-static analysis.

TABLE I
VELOCIROACH PARAMETERS

m	47.3 g (62.7 g)	l_1	1.5 cm
l	10 cm	l_2	2 cm
h	3 cm	h_1	2 cm
l_g	5.2 cm (5.3 cm)	r	2 cm
h_g	2.0 cm (2.1 cm)	δ	0.5 cm

locomotion performance, we determine the minimum tractive coefficient of friction required for either a single robot or two connected robots to remain in equilibrium at each possible configuration that could occur during step climbing, with robot/obstacle geometry and possible leg velocities providing additional constraints. This analysis predicts the success of two different primitives of the cooperative step climbing behavior: a single robot transitioning up a tall step in primitive I, and the connected robots climbing together to raise the front robot over the step in primitives III and IV.

A. Robot model

In the quasi-static analysis of step climbing, each legged robot is modeled in the sagittal plane as a single rigid body with three C-shaped legs whose tips follow trajectories parameterized by a single crank angle ϕ, based on the VelociRoACH transmission kinematics reported in [2]. This model is depicted in the diagram in Fig. 2. Although the modeled robot system has two motors that independently drive left and right leg sets, we restrict leg motion to in-phase bounding gaits in order to reduce the effect of roll and yaw motions on the accuracy of the pitch plane analysis. At the crank angle $\phi = 90^\circ$ shown, driving the motors moves the outer legs backwards to propel the robot forward, while moving the middle legs forward to prepare for the next step. The robot has mass m, body length l, body height h, center of mass distance l_g from the back of the robot body, center of mass height h_g from the bottom of the robot body, and body shape dimensions l_1, l_2, and h_1. Each C-leg has length r and is offset a distance δ from the rotation point in the sagittal plane. Measured values for a VelociRoACH are given in Table I; values in parentheses indicate the parameter with the addition of the winch module.

B. Quasi-static force analysis

The analysis of step climbing is formulated as a quasi-static manipulation problem in the sagittal plane. This approach aims to accommodate system-level climbing robot design with a simplified template, as opposed to the more complex anchor model of dynamic six-legged self-manipulation presented by Johnson and Koditschek [29]. The free body diagrams for a single robot and for two connected robots in this formulation are shown in Fig. 3a and Fig. 3b. In the free body diagrams shown, the robots are climbing a step of height H and quasi-statically feasible configurations have ground contact at the back and step contact at the front. In the single robot case, the one configuration parameter is the pitch angle of the front robot, θ_2. In the two robot case, the configuration parameters are the height of the center of mass (C.o.M.) of the front robot, y_{g2}, and θ_2. The back robot has pitch angle θ_1 and forms a pin connection with the front robot that has torsional spring constant k_t and exerts no moment when $\theta_2 - \theta_1 = \theta_0$. The force and moment balance is performed in the right handed Cartesian basis $\{\mathbf{E_1}, \mathbf{E_2}, \mathbf{E_3}\}$.

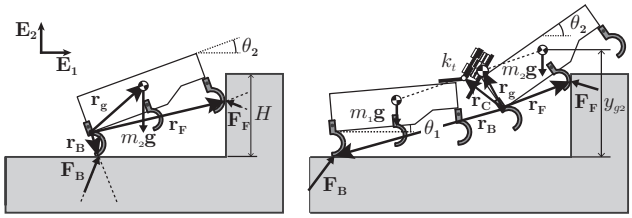

(a) (b)

Fig. 3. Free body diagram of (a) single robot step climbing and (b) two robot step climbing with a compliant pin connection between robots.

The forces that act on the system are gravity and contact forces against the ground and the step obstacle. Gravity acts vertically downward at the C.o.M. of each robot $m_i\mathbf{g} = -m_i g\mathbf{E_2}$, $g = 9.81$ ms^{-2}. Back contact force $\mathbf{F_B}$ and front contact force $\mathbf{F_F}$ act at contact displacements $\mathbf{r_B}$ and $\mathbf{r_F}$ respectively, relative to an origin at the back left corner of the front robot. The force balance for the two robot case is performed on the system of connected robots, with the internal forces of the connection not appearing. The same balance equations hold for both the single robot and two connected robot cases. In the single robot case, the system mass $m = m_2$ and the C.o.M. displacement vector $\mathbf{r_g}$ points towards the center of mass of the front robot. In the two connected robot case $m = m_1 + m_2$ and $\mathbf{r_g}$ is the mass weighted average of the C.o.M. positions of the front and back robot.

In each configuration, the contact displacements $\mathbf{r_B}, \mathbf{r_F}$, and normal vectors pointing away from the contact surface $\mathbf{N_B}, \mathbf{N_F}$ are determined as a function of the configuration parameters $[y_{g2}, \theta_2]$, the leg crank angle of each robot ϕ_i, and the geometry parameters of each robot $[l, h, l_1, l_2, h_1, r, \delta]_i$. These equations involve a set of inequality constraints that determine which leg (or part of the body) contacts the step obstacle and the valid horizontal distance of the front robot from the step in order to prevent collision with the step obstacle. From the contact normal vectors, tangent vectors $\mathbf{T_B}$ and $\mathbf{T_F}$ are computed such that $\mathbf{T_B} \times \mathbf{N_B} = \mathbf{E_3}$ and

$\mathbf{T_F} \times \mathbf{N_F} = \mathbf{E_3}$.

For each set of contact displacements and normal vectors, a friction-limited force and moment balance is solved to determine quasi-static limits on step climbing. The vector force balance (1) and moment balance about the center of gravity (2) are given below:

$$\mathbf{F_B} + \mathbf{F_F} - m\mathbf{g} = \mathbf{0} \quad (1)$$

$$(\mathbf{r_B} - \mathbf{r_g}) \times \mathbf{F_B} + (\mathbf{r_F} - \mathbf{r_g}) \times \mathbf{F_F} = \mathbf{0} \quad (2)$$

For the single robot case, there are three independent equations and four unknowns, two components each for $\mathbf{F_B}$ and $\mathbf{F_F}$, which yields infinitely many solutions. Assuming that there is an equal limiting coefficient of friction μ at the back and front contacts as a limiting case, we impose the two friction constraints $\mathbf{F_B} \cdot \mathbf{N_B} = \pm\mu \mathbf{F_B} \cdot \mathbf{T_B}$ and $\mathbf{F_F} \cdot \mathbf{N_F} = \pm\mu \mathbf{F_F} \cdot \mathbf{T_F}$. As shown in Fig. 3a, this places the contact forces at the edges of friction cones with the same internal angle. Adding these two constraints while introducing an unknown μ reduces the number of unknowns in the system of equations to three, which means there is at most one solution per branch for $||\mathbf{F_B}||$, $||\mathbf{F_F}||$, and μ.

For the two robot case, an additional equation from the torsion spring at the pin connection uniquely specifies contact forces for a given configuration. Performing a moment balance on the front robot about the pin connection yields the constitutive equation

$$(\mathbf{r_F} - \mathbf{r_C}) \times \mathbf{F_F} - m_2 (\mathbf{r_{g2}} - \mathbf{r_C}) \times \mathbf{g} = k_t (\theta_2 - \theta_1 - \theta_0)$$

where $\mathbf{r_C}$ is the displacement vector to the pin connection center, and $\mathbf{r_{g2}}$ is the C.o.M. displacement of the front robot.

The quasi-static analysis is used to determine friction limits on step climbing. Any solutions that cause collisions or require adhesion pulling into contact surfaces are disallowed. The limiting coefficients of friction are $\mu_{B,lim} = \frac{\mathbf{F_B} \cdot \mathbf{T_B}}{\mathbf{F_B} \cdot \mathbf{N_B}}$ at the back contact and $\mu_{F,lim} = \frac{\mathbf{F_F} \cdot \mathbf{T_F}}{\mathbf{F_F} \cdot \mathbf{N_F}}$ at the front contact. For the cases shown in Fig. 3, both contact forces indicate a sticking contact with propulsion in order to advance up the step. In this case, the limiting positive μ is a minimum tractive coefficient of friction. If either contact force is reflected about the normal, the condition would be changed to a sliding contact in order to advance up the step. In this case, the limiting negative μ is a maximum sliding coefficient of friction. Therefore, the four cases are: back and front propelling, back propelling and front sliding, back sliding and front propelling, and back and front sliding.

In the following quasi-static results for a single robot and two connected robots, a high traction obstacle is considered with $\mu_s = 1$, $\mu_k = 0.6$, where μ_s and μ_k are the measured static and dynamic coefficients of friction of a VelociRoACH leg on sandpaper. The leg angles are fixed at $\phi_i = 90°$ for simplicity of analysis.

C. Quasi-static single robot step climbing

For single robot step climbing, we allow each of the four combinations of sticking/sliding contacts, and fix the leg crank angle at $\phi = 90°$. For these conditions, Fig. 4 shows

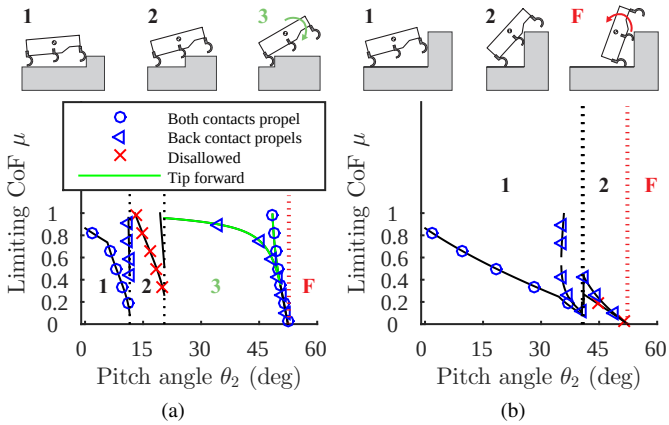

Fig. 4. Limiting coefficient of friction μ for single robot step climbing as a function of front robot pitch angle θ_2. (a) For a 2 cm step, a single robot can climb over the step if it performs beyond quasi-static limits. (b) For a 6.5 cm step, a single robot can transition to an increased angle but cannot climb over the step.

the limiting coefficient of friction for climbing a short step $H = 2$ cm and a tall step $H = 6.5$ cm. The regions 1, 2, 3 indicate when the front, middle, or back leg is contacting the step obstacle.

In the case of climbing a short step of $H = 2$ cm, the robot starts horizontally at $\theta_2 = 0°$. In order to quasi-statically progress, both the front and back legs need to propel the robot and the robot requires the largest tractive coefficient of friction at the start of climbing. In region 1, the static friction coefficient $\mu_s = 1$ satisfies the limit given in this plot. As the robot's inclination angle increases and its middle leg contacts the step, the robot cannot quasi-statically progress because it requires a propulsive contact that the middle leg kinematics cannot support. If the robot dynamically climbs the step, losing contact at the wall intermittently, it may be able to reach the green goal state in region 3. In this region, gravity will tend to passively tip the robot forward onto the step. This result is in contrast to a tracked vehicle, which can climb a comparable sized step without violating the quasi-static assumption due to continuous propulsive contact between a powered tread and the step.

In the case of climbing a tall step of $H = 6.5$ cm, the robot can quasi-statically pitch itself up the wall in region 1, because $\mu_s = 1$ is always greater than the tractive coefficient of friction limit. The middle leg comes into contact with the wall in region 2 at a larger pitch angle. In the case that the back contact propelling and the front contact is sliding, the robot can quasi-statically increase its pitch angle, but only in the range of angles in which the limiting coefficient of friction μ is less than the static friction $\mu_s = 1$ and above the dynamic friction $\mu_k = 0.6$ of the step obstacle. In this case, the step cannot be quasi-statically climbed because there is no configuration with ground and wall contact that puts the C.o.M. of the robot over the ledge. Therefore, the analysis predicts that quasi-statically, the robot should be able to increase its pitch angle to $40°$ before becoming stuck on its middle leg. Furthermore, in both the small step and large

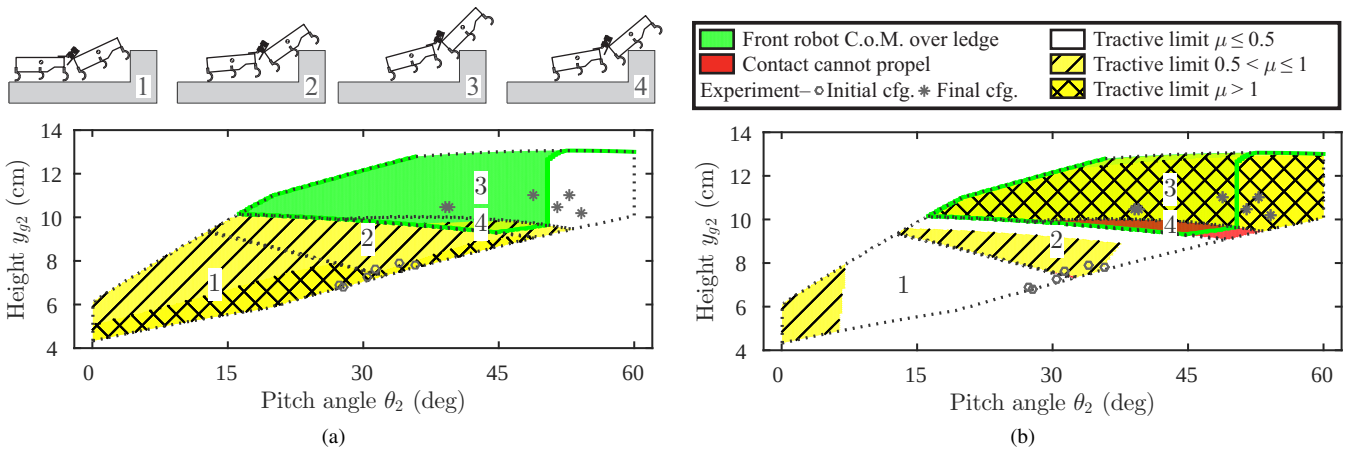

Fig. 5. Tractive coefficient of friction limits on two-connected-robot step climbing for the (a) back robot and (b) front robot. The dotted regions labeled 1, 2, 3, 4 indicate the wall contact configurations of the front robot. The green regions indicate successful end conditions in which the front robot will tend to passively tip forward when the connection between robots is released. Contact conditions within the region bounds can require low ($\mu \leq 0.5$, white), medium ($0.5 < \mu \leq 1$, yellow single hatched), or high ($\mu \geq 1$, yellow cross hatched) tractive coefficients of friction. The red regions show infeasibility due to inability to provide propulsion when the body contacts the wall. The markers show the initial (circles) and final (asterisks) configurations of successful connected climbing experiments.

step cases, if the dynamic effects of leg contact cause the robot's pitch angle to reach region F, its C.o.M. is behind the ground contact and gravity will pitch the robot onto its back, which is a failure state observed in Section IV.

D. Quasi-static connected robot step climbing

For two-connected-robot step climbing, the robots can have two independent bounding gaits, which means the outer legs of the back robot can propel the system at the same instance as the middle legs of the front robot. This added actuated degree of freedom enables the connected robots to climb a step that a single robot cannot climb. The connection parameters are set at a stiffness of $k_t = 0.018$ Nm/rad and a neutral angle of $\theta_0 = 30°$.

Figure 5 shows regions in the configuration space of front robot C.o.M. height y_{g2} and pitch angle θ_2 with different tractive coefficient of friction requirements on two-robot-connected climbing for the back robot (Fig. 5a) and front robot (Fig. 5b) quasi-statically climbing a step of height $H = 6.5$ cm. The dotted regions 1, 2, 3, 4 indicate whether the front leg, middle leg, back leg, or body of the front robot is contacting the step obstacle. The green region indicates success configurations for two robot connected step climbing.

We can draw several insights from this analysis on success conditions for two-connected-robot step climbing. Firstly, for this robot system, low traction steps are difficult to climb. The friction limits in Fig. 5 show that there are no sets of configurations with $\mu \leq 0.5$ starting from front or middle leg contact of the front robot that can reach the set of goal states. The legs of the back or front robot will slip when attempting to advance the connected robots up a low traction step.

Secondly, the high tractive coefficient of friction ($\mu > 1$) required of the back robot at small values of y_{g2} and θ_2 indicate that performing primitives I and II to pitch up and raise the center of mass of the front robot helps reach an initial configuration with $0.5 < \mu \leq 1$ from which propulsion from the back robot can advance the robots up a sandpaper step. This claim is supported by the fact that the estimated initial configurations during successful connected climbing experiments are near the boundary between the single hatched and cross hatched regions in Fig. 5a.

Finally, for a high-traction sandpaper step, the quasi-static analysis partially predicts the success of connected climbing (III) and connection release (IV) primitives. In traversing from the initial to final configurations in the connected climbing experiments, the analysis predicts that during middle leg contact of the front robot with a sandpaper step, the static friction $\mu_s = 1$ is sufficient for the back and front robot to propel the system. The quasi-static analysis cannot predict passing through the red region of sustained body contact, which can be explained by dynamic effects propelling the system past this sticking region. The final configurations in Fig. 5 should result in the front robot disconnecting on top of the step because the strategy for primitive IV involves the back robot pitching upward to pitch the front robot forward with its middle leg clear above the step, which moves the system configuration into the green success region.

Although quasi-statics predicts the robot will get stuck in certain regions shown in Fig. 5, dynamic effects (not yet modeled), can be used in practice to successfully climb the step as discussed in Section IV.

IV. Robot System and Experiments

The proposed two-robot team for cooperatively climbing step obstacles is shown in Fig. 6. The base robot platform is VelociRoACH, a 47 g, 10 cm long bio-inspired legged robot [2]. On each side of the robot, a brushed DC motor (3.6Ω pager motor) with a 64:1 reduction spur gear transmission drives an SCM kinematic linkage made of PET and Nylon and produces leg trajectories shown in Fig. 2.

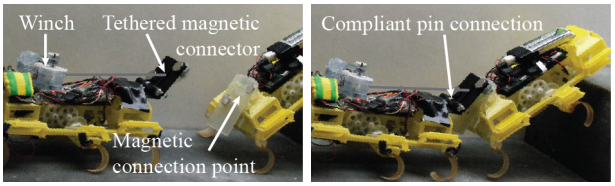

(a) (b)

Fig. 6. Team of two VelociRoACH robots with a compliant connection formed using a winch module on the back robot. (a) Forming a connection begins with a magnetic connector tethered to the back robot. (b) Magnets engage to form a compliant pin connection between robots.

The back robot is outfitted with a rapidly-prototyped winch module, which is used to tension the tether between the two robots. The winch tether is attached to a magnetic connector, which can be retained by the back robot (Fig. 6a). When the magnetic connector joins the robots together with a compliant pin connection (Fig. 6b) the back robot can exert a pushing force on the front robot, and a bending spring torque is produced between the robots as their relative angle deviates from the neutral angle $\theta_0 = 30°$. Additionally, the magnetic connector can be tethered to the front robot. In this case, the winch can pull the tether to assist climbing of the back robot. If the winch exerts a load on the tether exceeding a breaking load, the back robot retrieves the magnetic connector.

A. Winch module

An annotated picture of the rapidly prototyped winch module is shown in Fig. 7a. The winding and unwinding of the tether is driven by a brushed DC motor (3.6Ω pager motor) with a 60:1 reduction worm gear transmission. The tether material is 0.13 mm diameter polyethylene monofilament. The winch module weighs 10 g and can provide tensile forces up to 2.2 N at stall. The winch module maintains an applied tensile load using a load cell, as shown in Figs. 7b and 7c. To detect tether tension, an IR sensor (Sharp GP2S60B) measures the displacement of a spring-loaded four-bar platform upon which the winch module is mounted.

B. Cooperative step climbing experiments

Five sets of experiments independently testing each step climbing cooperation primitive in Fig. 1 were performed with the team of two VelociRoACH robots shown in Fig. 6. In the experiments, the robots were placed on a 6.5 cm step obstacle in a low-friction 11 cm wide channel (robot width is 6 cm) to limit yaw motions. The sandpaper step had a measured static coefficient of friction of $\mu_s = 1$ against the VelociRoACH legs. Although the experiments did not chain together the primitives in a single trial, the robots started flat on the bottom of the step, and the initial conditions of each primitive experiment were kept close to the final conditions of the preceding primitive experiment.

Figure 8 summarizes the reliability of cooperative step climbing experiments. Using a simple strategy of commanding a stride frequency and tether tension for each primitive resulted in success in at least 50% of trials for each of the five primitives performed independently. The success conditions

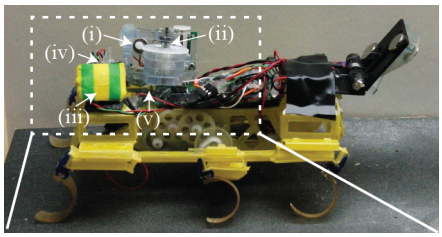

(a)

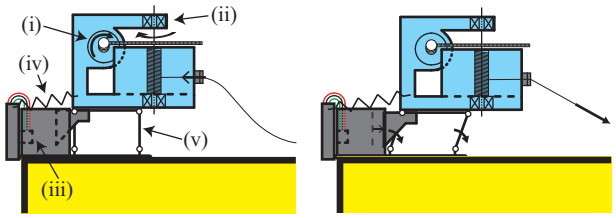

(b) (c)

Fig. 7. (a) Picture of the winch module on the robot with features highlighted: (i) Drive motor with worm gear meshed with spur gear on spool shaft, (ii) Bearing-supported spool shaft, (iii) Shrouded IR sensor, (iv) Restoring spring, (v) Compliant four-bar platform. Side view diagrams showing operation of the winch module under control to maintain tether tension: (b) When the tether is slack, the motor drives the spool to reel the tether in with no load registered by the IR sensor. (c) When the tether becomes taut, the platform displaces, stretching the spring, and the IR sensor registers increasing load based on increased distance to the reflector. When the desired tether tension has been reached, the motor stops rotating, which locks the worm transmission.

for transitioning to the next primitive were used as guidelines for valid initial conditions for the independent experiment set of each primitive.

Robot telemetry data for a representative set of successful trials is shown in Fig. 9. Refer to the video attachment for the experimental footage. The pitch angle of each robot is calculated using the initial accelerometer reading and forward integration of the gyroscope data. The winch load data is computed from a calibration of the IR sensor distance reading. The data sets are filtered using a moving average with a 200 ms window. This telemetry data along with the video illustrate the robots' behavior during successful trials of cooperative step climbing experiments.

In primitive I, the magnetic connector is secured on the back robot and does not impede the motion of the front robot as it bounds at 5 Hz at the base of the step. The success condition of the front robot pitched up against the step is predicted by the friction limited quasi-static analysis of single robot step climbing in Fig. 4b. The most common failure mode (3/10 trials) was the front robot pitching onto its back.

In primitive II, the back robot forms a compliant pin connection with the front robot by maintaining a set tether tension while walking forward. The front robot raises its magnetic connection point upward to join to the magnetic connector on the back robot. At the start of the experiment, the back robot starts aligned in yaw and directly behind the front robot. This primitive had the highest success rate of 9/10. The one failure was due to misalignment of the magnetic connection.

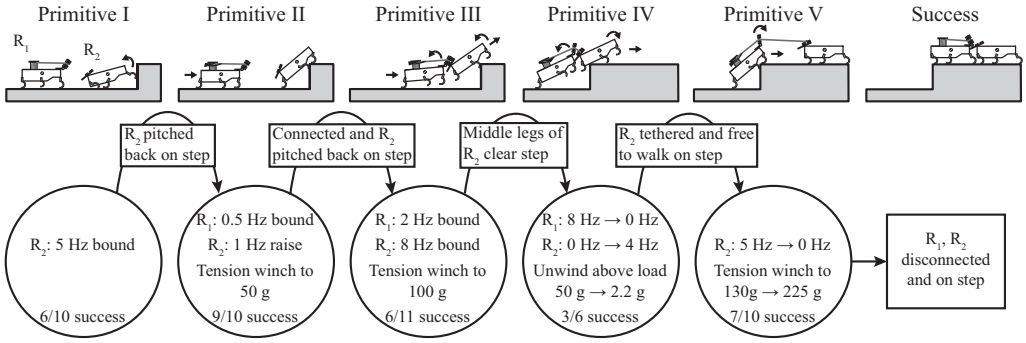

Fig. 8. Experimental reliability of step climbing cooperation primitives. For each primitive performed independently for multiple trials with feasible initial conditions, each bubble shows the open-loop stride strategy and winch load used, as well as the success rate. The boxes show success conditions for transitioning between sequential primitives.

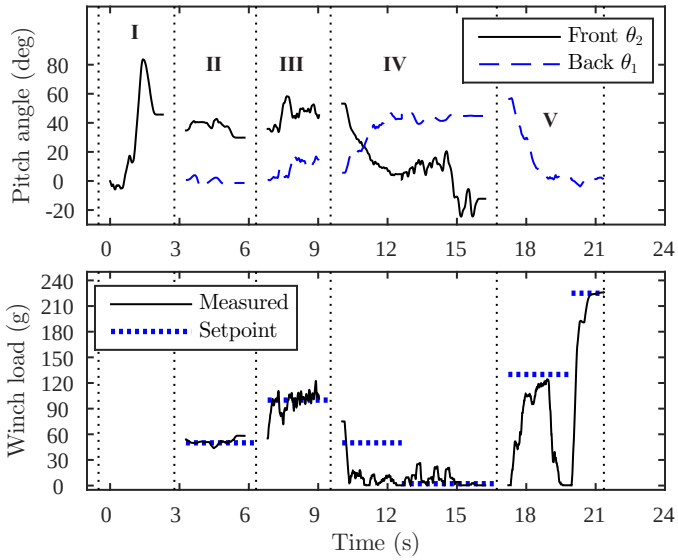

Fig. 9. Telemetry data for representative successful cooperative step climbing experiments. Primitives (I) - (V) were performed independently.

In primitive III, the back robot maintains the compliant connection with a set tether tension while running slower than the front robot. This gait strategy produces switched propulsive contact of middle and back legs of the front robot as the back robot pushes with its back legs to raise the middle leg of the front robot over the step. The initial and final pitch configurations of these experiments plotted in Fig. 5 partially agree with the quasi-static analysis. The analysis correctly predicts that the propulsion of the back robot on the ground combined with the middle legs of the front robot on the step can advance the system. However, the dynamic bounding gait of 8 Hz produces intermittent step contact, as is shown in the experimental video, which can explain the system moving past configurations with body contact against the step. The only failure mode in this experiment was the front robot twisting about the connection, which resulted in its middle legs getting stuck on the step.

In primitive IV, the back robot releases the pin connection by relaxing the tether tension above loads of 50 g as it bounds at 8 Hz to pitch the front robot forward. This primitive is successful when the front robot can run forward past the edge of the step with the tethered magnetic connector attached. The back robot permits forward motion of the front robot by reeling out the tether above loads of 2.2 g. This result is predicted by the quasi-static analysis because the pushing motion of the back robot while reeling out the tether acts to drive the final configurations of primitive III plotted in Fig. 5 towards the green success region. This primitive had the lowest success rate of 3/6, and the failure mode was the front robot tipping backwards off the step due to insufficient pushing support by the back robot.

In primitive V, the back robot climbs the step while assisted by a tether pulling force. The tethered magnetic connector is attached to the front robot, which has its legs hooked around a ledge feature at the end of the step to prevent from slipping. The previous primitive leaves the back robot pitched against the step. The winch pulls with a load setpoint of 130 g while the robot runs with a stride frequency of 5 Hz and the magnetic connector remains on the front robot. This pitches the back robot forward and over the edge of the step, stopping against the front robot. The robot then retrieves the magnetic connector by applying a tether tension past a breaking load. In 2/10 experiments, the back robot failed to climb the step because its middle legs were stuck against the step. In 1/10 experiments, the back robot failed to retrieve the magnetic connector due to misalignment.

V. Discussion

In conclusion, we have demonstrated that a system of two underactuated legged robots with a removable connection driven by one additional actuator can perform cooperation primitives that result in both robots climbing over a 6.5 cm tall step. The quasi-static analysis predicts the success of the first robot to change to a pitched-up posture on the step before forming the connection to the robot with the winch module (primitive I). The analysis also partially predicts the success of the cooperative climbing behavior in raising the front robot on top of the step (primitives III and IV). In future work, quasi-static friction limits along with iterative design can produce geometry, leg kinematics,

and connection parameters of cooperative robot systems that are suited for climbing steps of varying height and friction. Additionally, dynamic strategies for cooperative step climbing can be modeled and implemented to overcome the observed limitations of quasi-statics.

Utilizing sensory information to move beyond the simple strategies for executing each primitive could increase the overall success rate of cooperative step climbing. Although each primitive was successfully performed with at least a 50% success rate, assuming each chained together primitive is independent results in a predicted overall success rate of 10%. Pose estimates from IMU information and motor torque measurements could be combined to adjust the control of leg and winch motions to move the robot team over the step in a more predictable manner. Forming and releasing the connection (primitives II and IV) could benefit from contact sensors detecting whether the magnetic connector is retained by the back robot, attached to the front robot, or fixed to the compliant pin connection between robots. In forming the connection, alignment of the two robots is important for success, so detection of relative heading and distance of the robots could also be useful.

Another limitation of the experimental system is that it was necessary to restrict the yaw of the robots in order to successfully climb the step. Incorporating a yaw controller to stabilize the robots, especially in the connected climbing mode (primitive III) with observed dynamic effects is important for demonstrating this system beyond a laboratory environment.

Finally, in tether-assisted climbing (primitive V), we assumed that the front robot can always find an anchoring point to support the back robot's tether pulling loads. In the future, the addition of an attachment mechanism to the front robot, or having the front robot search for an anchoring point in the environment could help both robots climb obstacles in real-world environments.

ACKNOWLEDGMENT

The authors would like to thank the members of the Biomimetic Millisystems Laboratory for valuable discussions.

REFERENCES

[1] A. M. Hoover and R. S. Fearing, "Fast scale prototyping for folded millirobots," in *IEEE ICRA*, May 2008, pp. 886–892.

[2] D. W. Haldane, K. C. Peterson, F. L. Garcia Bermudez, and R. S. Fearing, "Animal-inspired design and aerodynamic stabilization of a hexapedal millirobot," in *IEEE ICRA*, May 2013, pp. 3279–3286.

[3] A. O. Pullin, N. J. Kohut, D. Zarrouk, and R. S. Fearing, "Dynamic turning of 13 cm robot comparing tail and differential drive," in *IEEE ICRA*, 2012.

[4] D. W. Haldane and R. S. Fearing, "Roll oscillation modulated turning in dynamic millirobots," in *IEEE ICRA*, May 2014, pp. 4569–4575.

[5] P. Birkmeyer, A. G. Gillies, and R. S. Fearing, "CLASH: Climbing vertical loose cloth," in *IEEE/RSJ IROS*, Sep. 2011, pp. 5087–5093.

[6] M. Spenko, G. Haynes, J. Saunders, M. Cutkosky, A. Rizzi, R. Full, and D. Koditschek, "Biologically inspired climbing with a hexapedal robot," *Journal of Field Robotics*, vol. 25, no. 2008, pp. 223–242, 2008.

[7] G. A. Lynch, J. E. Clark, P.-C. Lin, and D. E. Koditschek, "A bioinspired dynamical vertical climbing robot," *The International Journal of Robotics Research*, vol. 31, no. 8, pp. 974–996, Apr. 2012.

[8] S. Kim, M. Spenko, S. Trujillo, B. Heyneman, D. Santos, and M. R. Cutkosky, "Smooth vertical surface climbing with directional adhesion," *IEEE Transactions on Robotics*, vol. 24, no. 1, pp. 65–74, 2008.

[9] P. Birkmeyer, A. G. Gillies, and R. S. Fearing, "Dynamic climbing of near-vertical smooth surfaces," in *IEEE/RSJ IROS*, Oct. 2012, pp. 286–292.

[10] M. P. Murphy and M. Sitti, "Waalbot: An agile small-scale wall-climbing robot utilizing dry elastomer adhesives," *IEEE/ASME Transactions on Mechatronics*, vol. 12, no. 3, pp. 330–338, 2007.

[11] M. P. Murphy, C. Kute, Y. Menguc, and M. Sitti, "Waalbot II: Adhesion recovery and improved performance of a climbing robot using fibrillar adhesives," *The International Journal of Robotics Research*, vol. 30, no. 1, pp. 118–133, Oct. 2010.

[12] G. Caprari, A. Breitenmoser, W. Fischer, C. Hürzeler, F. Tâche, R. Siegwart, O. Nguyen, R. Moser, P. Schoeneich, and F. Mondada, "Highly compact robots for inspection of power plants," *Journal of Field Robotics*, vol. 29, no. 1, pp. 47–68, 2012.

[13] M. Bonani, S. Magnenat, P. Rétornaz, and F. Mondada, "The handbot, a robot design for simultaneous climbing and manipulation," in *Intelligent Robotics and Applications*. Springer, 2009, pp. 11–22.

[14] Y.-C. Chou, W.-S. Yu, K.-J. Huang, and P.-C. Lin, "Bio-inspired step-climbing in a hexapod robot," *Bioinspiration and Biomimetics*, vol. 7, no. 3, p. 036008, Sep. 2012.

[15] A. D. Deshpande and J. E. Luntz, "A methodology for design and analysis of cooperative behaviors with mobile robots," *Autonomous Robots*, vol. 27, no. 3, pp. 261–276, Jul. 2009.

[16] S. Shoval and A. Shapiro, "Dual-tracked mobile robot for motion in challenging terrains," *Journal of Field Robotics*, vol. 28, no. 5, pp. 769–791, 2011.

[17] K. Suzuki, A. Nakano, G. Endo, and S. Hirose, "Development of multi-wheeled snake-like rescue robots with active elastic trunk," in *IEEE/RSJ IROS*, Oct. 2012, pp. 4602–4607.

[18] J. Liu, Y. Wang, S. Ma, and B. Li, "Analysis of stairs-climbing ability for a tracked reconfigurable modular robot," in *IEEE International Workshop on Safety, Security and Rescue Robotics*, 2005, pp. 36–41.

[19] S. Avinash, A. Srivastava, A. Purohit, S. V. Shah, and K. M. Krishna, "A compliant multi-module robot for climbing big step-like obstacles," in *IEEE ICRA*, May 2014, pp. 3397–3402.

[20] H. Kimura and S. Hirose, "Development of Genbu: Active wheel passive joint articulated mobile robot," in *IEEE/RSJ IROS*, Oct. 2002, pp. 823–828.

[21] K. Ito and R. Murai, "Snake-like robot for rescue operations Proposal of a simple adaptive mechanism designed for ease of use," *Advanced Robotics*, vol. 22, no. 6-7, pp. 771–785, Jan. 2008.

[22] T. Seo and M. Sitti, "Tank-like module-based climbing robot using passive compliant joints," *IEEE/ASME Transactions on Mechatronics*, vol. 18, no. 1, pp. 397–408, 2013.

[23] J. Werfel, K. Petersen, and R. Nagpal, "Designing collective behavior in a termite-inspired robot construction team," *Science*, vol. 343, no. 6172, pp. 754–758, 2014.

[24] N. Napp and R. Nagpal, "Distributed amorphous ramp construction in unstructured environments," *Robotica*, vol. 32, no. 2, pp. 279–290, Feb. 2014.

[25] E. Mumm, S. Farritor, P. Pirjanian, C. Leger, and P. Schenker, "Planetary cliff descent using cooperative robots," *Autonomous Robots*, vol. 16, no. 3, pp. 259–272, 2004.

[26] J. Bares and D. Wettergreen, "Dante II: Technical description, results, and lessons learned," *The International Journal of Robotics Research*, vol. 18, no. 7, pp. 621–649, 1999.

[27] I. A. D. Nesnas, J. B. Matthews, P. Abad-Manterola, J. W. Burdick, J. A. Edlund, J. C. Morrison, R. D. Peters, M. M. Tanner, R. N. Miyake, B. S. Solish, and R. C. Anderson, "Axel and DuAxel Rovers for the Sustainable Exploration of Extreme Terrains," *Journal of Field Robotics*, vol. 29, no. 4, pp. 663–685, 2012.

[28] H. Schempf, "Self-Rappelling Robot System for Inspection and Reconnaissance in Search and Rescue Applications," *Advanced Robotics*, vol. 23, no. 9, pp. 1025–1056, Jan. 2009.

[29] A. M. Johnson and D. E. Koditschek, "Legged self-manipulation," *Access, IEEE*, vol. 1, pp. 310–334, 2013.